

1956

# Bucket-type energy dissipator characteristics, 1956

M. H. Karr

Follow this and additional works at: <http://preserve.lehigh.edu/engr-civil-environmental-fritz-lab-reports>

---

## Recommended Citation

Karr, M. H., "Bucket-type energy dissipator characteristics, 1956" (1956). *Fritz Laboratory Reports*. Paper 1712.  
<http://preserve.lehigh.edu/engr-civil-environmental-fritz-lab-reports/1712>

This Technical Report is brought to you for free and open access by the Civil and Environmental Engineering at Lehigh Preserve. It has been accepted for inclusion in Fritz Laboratory Reports by an authorized administrator of Lehigh Preserve. For more information, please contact [preserve@lehigh.edu](mailto:preserve@lehigh.edu).

F.L. Library Copy  
262

308

3512A  
262

FRITZ ENGINEERING LABORATORY  
LEHIGH UNIVERSITY  
DOTHLEHEM, PENNSYLVANIA

LEHIGH UNIVERSITY  
INSTITUTE OF RESEARCH  
PROJECT 1052-12

BUCKET-TYPE  
ENERGY DISSIPATORS

FRITZ ENGINEERING  
LABORATORY LIBRARY

Report For Course Credit  
In C.E. 421 - HYDRAULIC LABORATORY PRACTICE  
Department of Civil Engineering

by

Malcolm H. Karr

April 1956

April 16, 1956

Professor M. B. McPherson  
Dept. of Civil Engineering  
Lehigh University

Dear Professor McPherson:

This is a letter of submittal to you as Course Supervisor concerning Project 1052-12, BUCKET-TYPE ENERGY DISSIPATORS.

The following report is in partial satisfaction of requirements for C.E. 421, HYDRAULIC LABORATORY PRACTICE, as part of the graduate program leading towards a MS degree undertaken by the author at Lehigh University.

This report covers only the initial phase of the project and discusses only a part of the data obtained to date. The remainder of the data, as well as subsequent information, will be covered in a report for C.E. 422, HYDRAULIC RESEARCH, which will be submitted in June 1956.

Respectfully submitted

Malcolm H. Karr

MHK:EEY

## TABLE OF CONTENTS

	<u>Page</u>
Letter of Submittal	Frontispiece
Introduction	1
The Bucket Model	1
Hydraulic and Other Measurements	2
Results	2
Future Tests	4
Acknowledgments	5
Appendix	12

## ILLUSTRATIONS

Figure 1 - General View of Model Setup	6
Figure 2 - Definition Sketch	7
Figure 3 - Typical View of Bucket Section In Operation	8
Figure 4 - Parameter Plot ( $\frac{q}{\sqrt{g} h_2^{3/2}}$ vs. $\frac{h_b}{h_2}$ )	9
Figure 5 - Parameter Plot ( $\frac{h_b}{h_1}$ vs. $\frac{h_2}{h_1}$ )	10
Figure 6 - Parameter Plot ( $\frac{h_b}{h_1}$ vs. $\frac{h_s}{h_1}$ )	11

C.E. 421

BUCKET-TYPE ENERGY DISSIPATORS

~~PROJECT 1052-12~~

INTRODUCTION

As outlined in the tentative program for the Committee on Design, Hydraulics Division, ASCE (a copy of which is included in the Appendix), the major objective of this program is to determine parameter values for bucket-type energy dissipators of a specified class for direct use in design. The program was divided into various phases and this report, as well as most of the data obtained to date, apply almost entirely to Phase I.

THE BUCKET MODEL

The laboratory setup, with the bucket currently being tested ( $R = 1.2$  ft.) installed, is shown in the photograph of Fig. 1. The rate of flow and the initial head on the bucket are controlled by a sluice gate located at the upstream end of the approach channel, and the tailwater depth is controlled by a sluice gate located at the downstream end of the discharge channel. Both channels, as well as the bucket section, are of a constant width of 1 ft. The tailwater depth can be raised to a maximum of 6 ft.

Figure 2 is a definition sketch showing the nomenclature and symbols which will be used throughout this report.

Note that the approach channel is shown at a 45-degree angle with the horizontal, and that the discharge channel is shown horizontal. These slopes have been kept constant throughout the testing. Also, the angle of the tangent at the bucket lip with the horizontal has been maintained at 45 degrees. Figure 3 has been included to give a general picture of the model in operation.

#### HYDRAULIC AND OTHER MEASUREMENTS

Discharge measurements were made using a calibrated 8 by 4-in. Venturi meter in the supply line with an air-water manometer for the lower rates of flow and a mercury-water manometer for the higher ranges.

The depth of flow in the approach channel was determined using a point gage which read directly to 0.001 ft.

Other depth measurements were made directly with a scale during the run; from over the top of the channel for the initial bucket; from the side of the channel at present, since one side is now of Plexiglass for better visual determination of the various conditions of flow. All of the head measurements ( $h_1$ ,  $h_2$ ,  $h_b$ ,  $h_s$ ) are referred to the elevation of the bucket invert as zero datum.

RESULTS (The data used for the plots in this report are included in the Appendix)

1. For the combination  $\frac{q}{\sqrt{g} h_2^{3/2}} = \phi \left( \frac{h_1}{h_2}, \frac{h_b}{h_2}, \frac{R}{h_2} \right)$ ,

plots were made of the data obtained for a series of runs holding  $q$  and  $h_1$  constant for each series. Figure 4 is a plot of the  $q$  parameter vs.  $h_b/h_2$  and includes several of the series of runs for the initial bucket ( $R = 0.6$  ft.) as well as two series of runs for the present bucket ( $R = 1.2$  ft.). Note that a condition of spray or unsteady, pulsating surge, begins when the depth of the bucket,  $h_b$ , drops below 0.6 of the tailwater depth,  $h_2$ , and the jet springs free when  $h_b$  is less than  $0.2 h_2$ . This condition prevails for all cases and seems to be independent of both  $R$  and the value of the  $q$  parameter. The limiting case of  $h_b = h_2$  appears to be a function of the  $q$  parameter. Once that condition is reached, for a given  $q$ , further increase in tailwater depth merely causes a like increase in  $h_b$ .

2.(a) For the combination  $\frac{q}{\sqrt{g} h_1^{3/2}} = \phi \left( \frac{h_2}{h_1}, \frac{h_b}{h_1}, \frac{R}{h_1} \right)$ ,

plots were made for the same series of runs mentioned in 1, above. Figure 5 is a plot of  $h_b/h_1$  vs.  $h_2/h_1$  for various

$\frac{q}{\sqrt{g} h_1^{3/2}}$  values. Here again, the limiting value of  $h_b = h_2$

is reached by each series at a point dependent upon the value of the  $q$  parameter. The curves form a family of curves, the width of the band depending upon the range of  $\frac{q}{\sqrt{g} h_1^{3/2}}$  values.

Of significance is that the curves nearest to the line  $h_b = h_2$  are for the series of runs with the lowest  $\frac{q}{\sqrt{g} h_1^{3/2}}$  values and therefore represent the highest heads,  $h_1$ , while those

farthest from the same line have the highest  $\frac{q}{\sqrt{g} h_1^{3/2}}$  values.

Also shown on the plot are lines of  $h_b = 0.6h_2$  and  $h_b = 0.2h_2$ , which further exemplify and verify the spray and free-jet regions mentioned above.

(b) Figure 6 is a plot of  $h_b/h_1$  vs.  $h_s/h_1$  for the same runs as (a) above. This family of curves approaches the limiting value of  $h_b = h_s$ , at which point the surge is entirely submerged by the tailwater. This condition, relatively speaking, requires a very high tailwater. Of interest are the lines shown on the plot of  $h_b = 0.5h_s$  and  $h_b = 0.1h_s$ , which again define the spray and free-jet regions.

#### FUTURE TESTS

The results shown include only a part of the data, a good part of the work being done towards C.E. 422 credit, and the remainder of the data will be covered in a C.E. 422 report.

To complete the requirements of C.E. 422 (Spring Semester 1956), it is expected that additional information will be obtained on the present bucket ( $R = 1.2$  ft.) and, if time permits, a short study - using the glass-walled flume available in the laboratory - will be made in order to obtain data for a smaller  $h_1$  than can be produced with the present equipment. This would permit extending the range to larger values of the parameter  $\frac{q}{\sqrt{g} h_1^{3/2}}$ . (The data to date would apply to "high" or "medium-height" dams).

The following work cannot be covered under the Thesis program:



1. Most, if not all, of Phase II.
2. Phase III. However, data already taken on  $h_s$  and  $x_s$  should prove invaluable in scour study.
3. Variable upstream angle. (A chute model is available in the laboratory having a 33-degree approach angle. Performing check tests on the upstream angle would be first in order for an extension of this research program.

At the conclusion of the course work on this program, the following studies should be made immediately to complete Phase I and to initiate Phase II:

1. Completion of extension of data for large values of the parameter  $\frac{q}{\sqrt{g} h_1^{3/2}}$ , if necessary or desirable.
2. Short test on chute model with 33-degree approach angle to determine practicability of intensive program with a variable approach angle.
3. Correlation of data with limited, existing reference data.

#### ACKNOWLEDGMENTS

The tests reported were performed in the Hydraulics Laboratory of Fritz Engineering Laboratory. Supervision and mechanic assistance were provided from Department funds by authorization of Professor W. J. Eney, Head of the Department of Civil Engineering and Fritz Laboratory Director. Nearly all of the special materials used in this study (to June 1956) were provided by a Grant-In-Aid Fund of \$500 from the consulting firm of Gannett, Fleming, Corddry and Carpenter, Inc. The encouragement of Mr. William H. Corddry is gratefully acknowledged.

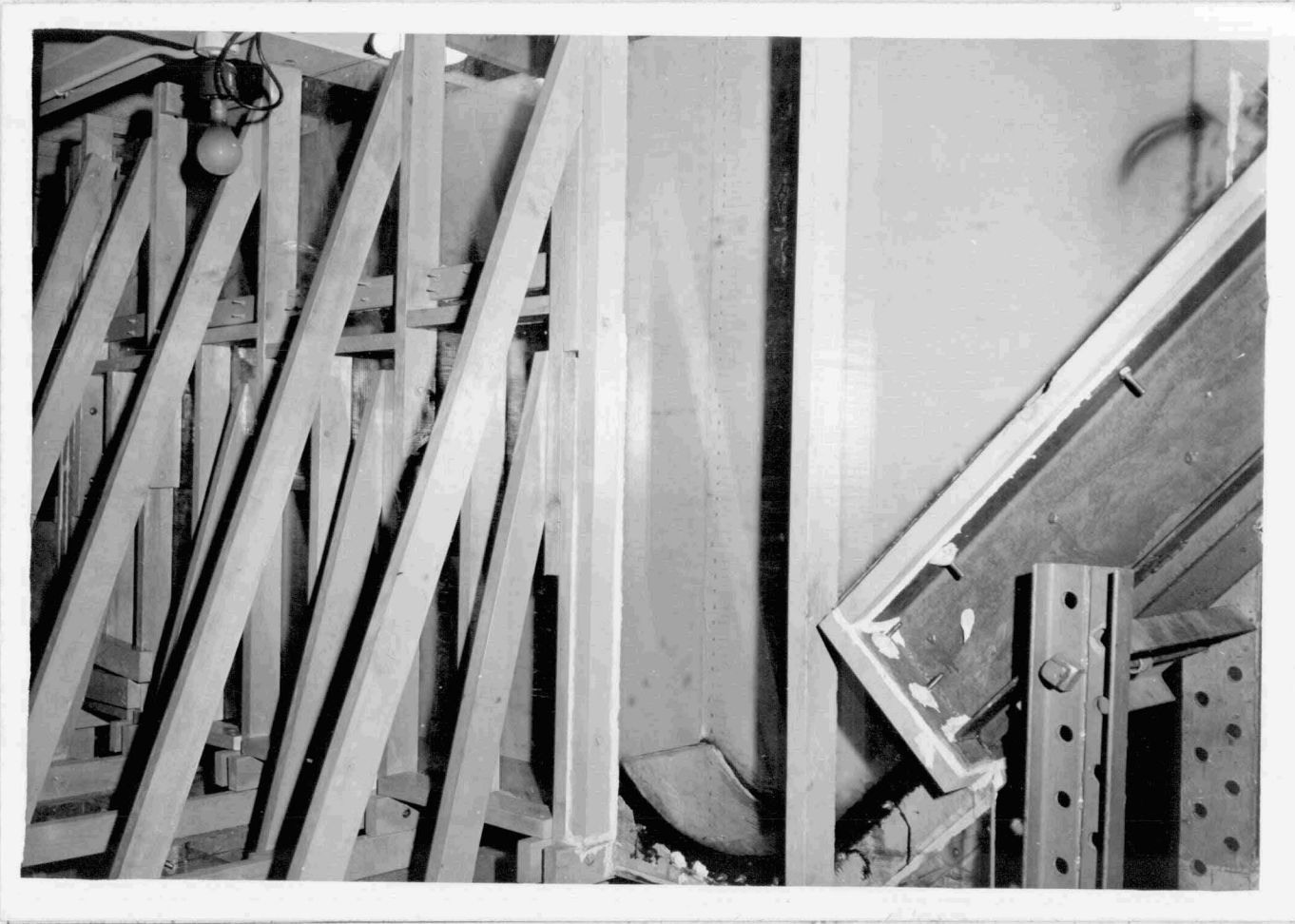


Figure 1 - General View of Model Setup,  
Bucket of  $R = 1.2$  ft, Installed

Nomenclature:

$h_1$  = Initial head on bucket  
 $h_b$  = depth of water in bucket  
 $h_s$  = height of surge  
 $h_2$  = tailwater depth

} All head measurements relative to bucket invert

$d$  = depth of flow in approach channel measured normal to channel bottom  
 $Z_d$  = height of depth measuring station above channel invert

$R$  = bucket radius

$x_s$  = distance from bucket lip to surge peak

$x_{scour}$  = distance from bucket lip to downstream end of scour pattern

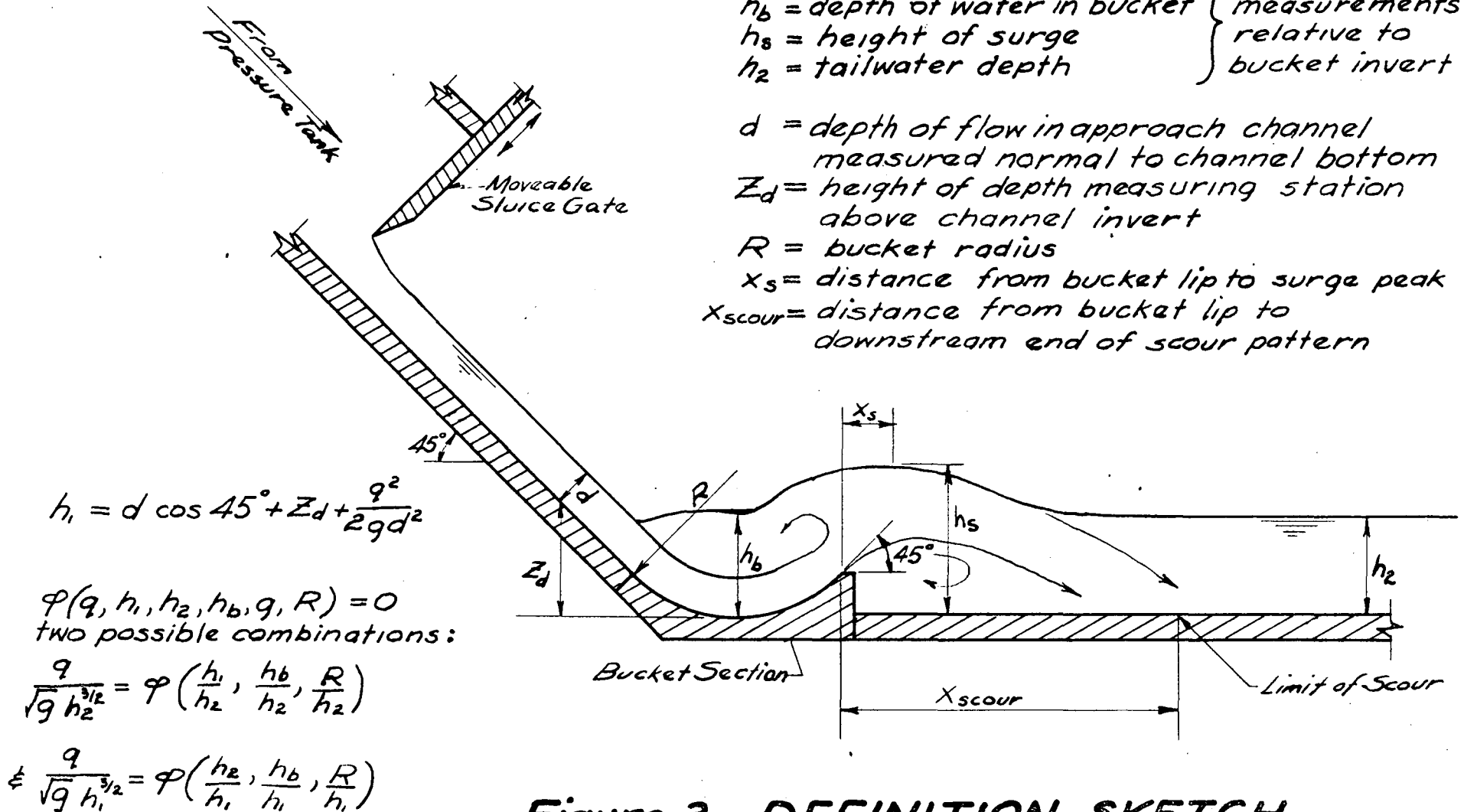
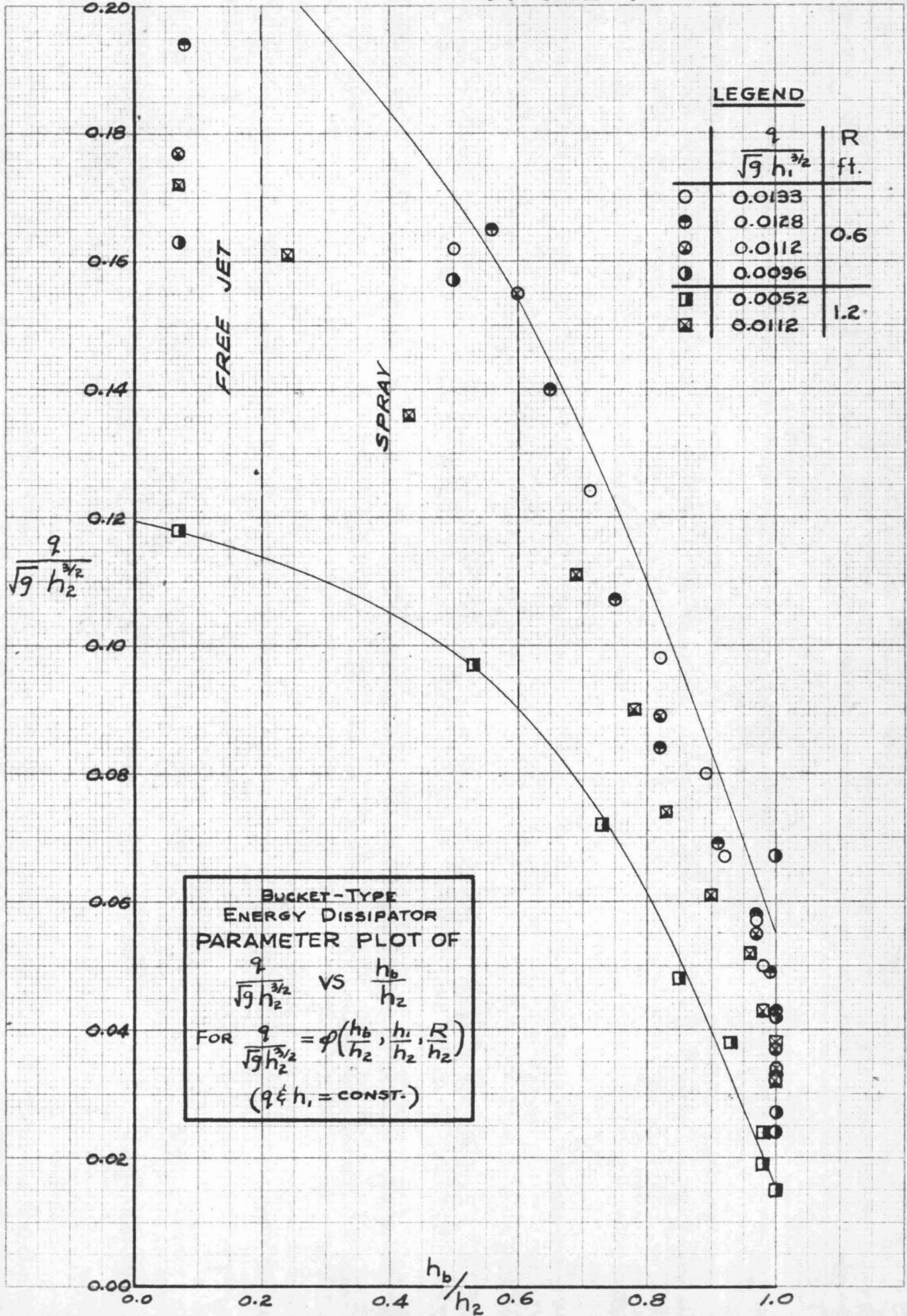


**Figure 2. DEFINITION SKETCH  
Bucket-Type Energy Dissipator**



Figure 3 - Typical View of Bucket Section in Operation  
(R = 1.2 ft.)

FIGURE 4



NO. 340R-20 DIETZGEN GRAPH PAPER  
 20 X 20 PER INCH  
 EUGENE DIETZGEN CO.  
 MADE IN U.S.A.



**BUCKET-TYPE  
 ENERGY DISSIPATOR  
 PARAMETER PLOT OF**  

$$\frac{h_b}{h_1} \text{ VS } \frac{h_2}{h_1}$$
**FOR** 
$$\frac{q}{\sqrt{g h_1^{3/2}}} = \varphi\left(\frac{h_b}{h_1}, \frac{h_2}{h_1}, \frac{R}{h_1}\right)$$
**( $q \neq h_1 = \text{CONST.}$ )**

NO. 340R-20 DIETZGEN GRAPH PAPER  
 20 X 20 PER INCH  
 EUGENE DIETZGEN CO.  
 MADE IN U.S.A.

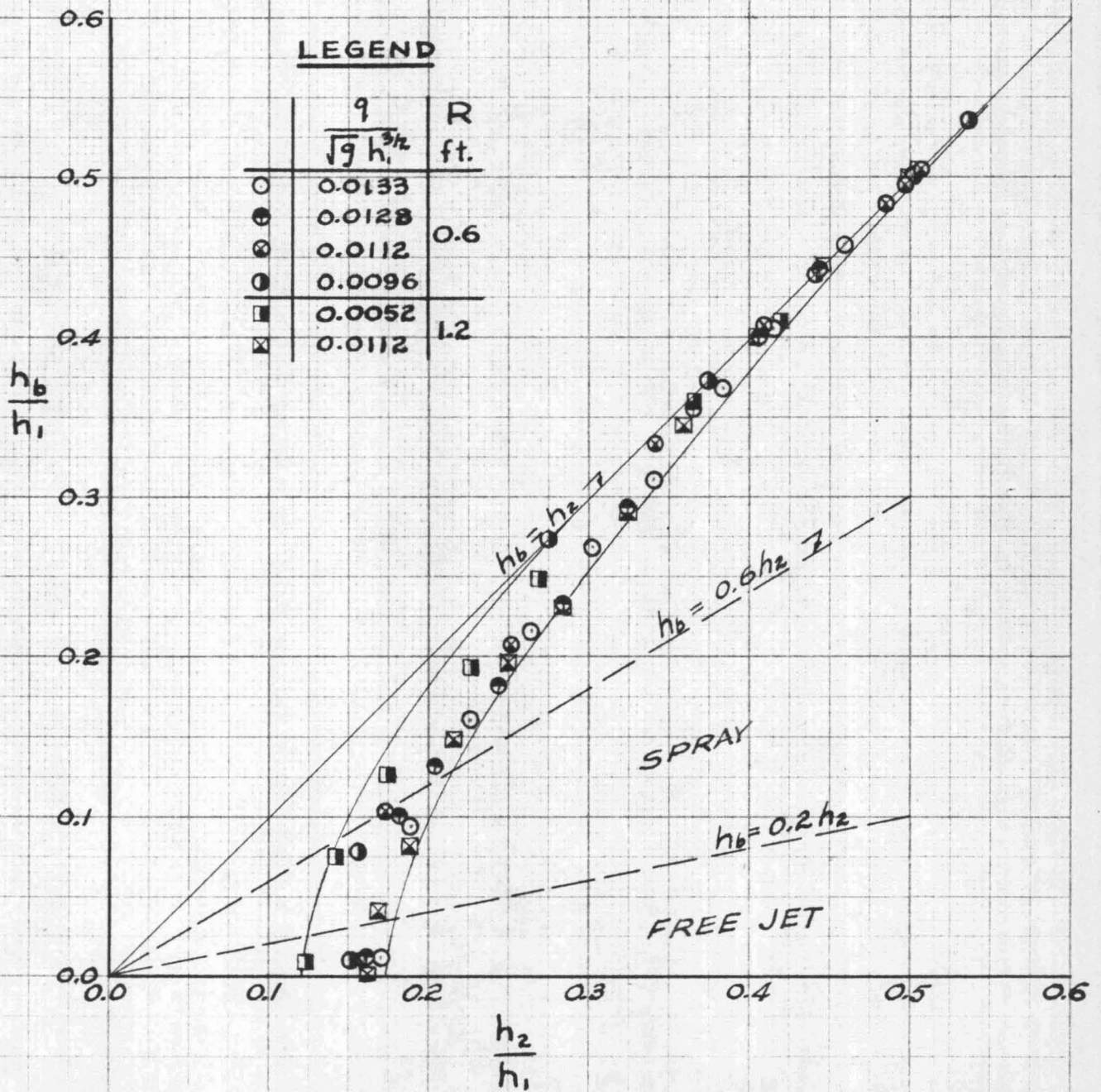


**FIGURE 5**

**BUCKET-TYPE  
ENERGY DISSIPATOR  
PARAMETER PLOT OF**  
 $\frac{h_b}{h_1}$  VS  $\frac{h_s}{h_1}$   
 FOR  $\frac{q}{\sqrt{g} h_1^{3/2}} = \varphi\left(\frac{h_b}{h_1}, \frac{h_2}{h_1}, \frac{R}{h_1}\right)$   
 ( $q \& h_1 = \text{CONST}$ )

**LEGEND**

	$\frac{q}{\sqrt{g} h_1^{3/2}}$	R ft.
○	0.0133	0.6
⊙	0.0128	
⊗	0.0112	
●	0.0096	
□	0.0052	1.2
⊠	0.0112	

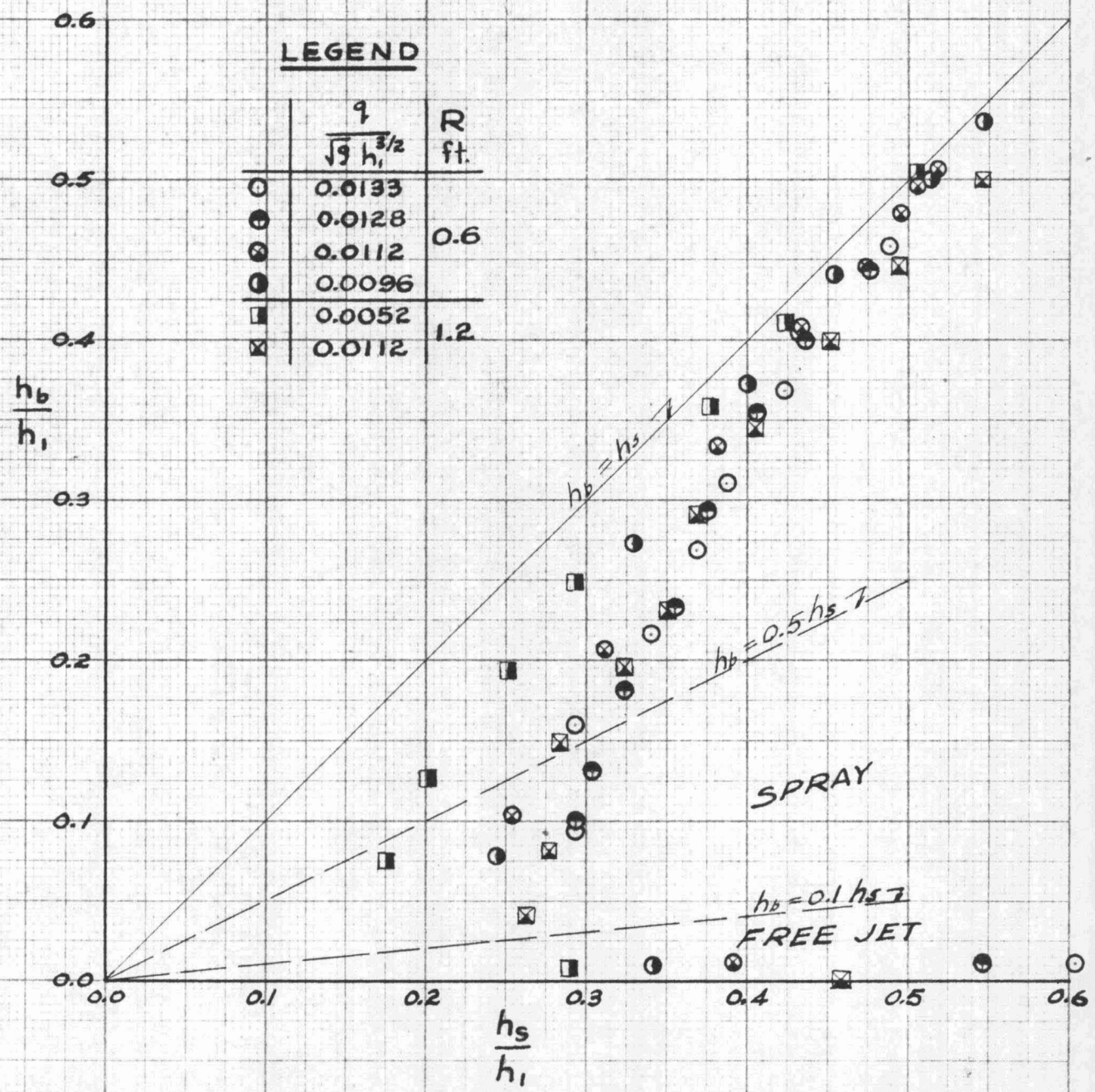


**FIGURE 6**

EUGENE DIETZGEN CO.  
MADE IN U.S.A.

NO. 340R-20 DIETZGEN GRAPH PAPER  
20 X 20 PER INCH

APPENDIX

Data for Plots of Figures 4, 5 & 6

R = 0.6 ft.

Run	$h_2$ ft.	$h_b$ ft.	$h_s$ ft.	$h_b/h_1$	$h_2/h_1$	$h_s/h_1$	$h_b/h_2$	$\frac{q}{\sqrt{g} h_2^{3/2}}$	Symbol on Plot
$q = 0.920$ cfs/ft.; $h_1 = 5.30$ ft.; $\frac{q}{\sqrt{g} h_1^{3/2}} = 0.0133$									
45	2.42	2.42	2.55	0.459	0.459	0.488	1.00	0.043	○
46	2.20	2.15	2.30	0.406	0.415	0.433	0.98	0.050	
47	2.00	1.95	2.24	0.368	0.378	0.423	0.97	0.057	
48	1.80	1.65	2.05	0.311	0.340	0.387	0.92	0.067	
49	1.60	1.42	1.90	0.268	0.302	0.369	0.89	0.080	
50	1.40	1.15	1.80	0.217	0.264	0.340	0.82	0.098	
51	1.20	0.85	1.55	0.160	0.226	0.293	0.71	0.124	
52	1.00	0.50	1.55	0.094	0.189	0.293	0.50	0.162	
*53	0.80	0.06	3.20	0.012	0.170	0.603	0.08	0.225	
$q = 0.794$ cfs/ft.; $h_1 = 4.93$ ft.; $\frac{q}{\sqrt{g} h_1^{3/2}} = 0.0128$									
57	2.19	2.19	2.35	0.443	0.443	0.477	1.00	0.043	○
58	2.00	1.97	2.15	0.400	0.406	0.436	0.99	0.049	
59	1.80	1.75	2.00	0.355	0.365	0.406	0.97	0.058	
60	1.60	1.45	1.85	0.294	0.324	0.375	0.91	0.069	
61	1.40	1.15	1.75	0.233	0.284	0.355	0.82	0.084	
62	1.20	0.90	1.60	0.182	0.243	0.324	0.75	0.107	
63	1.00	0.65	1.50	0.132	0.203	0.304	0.65	0.140	
64	0.90	0.50	1.45	0.101	0.182	0.294	0.56	0.165	
*65	0.80	0.06	2.70	0.012	0.162	0.547	0.08	0.194	
$q = 0.572$ cfs/ft.; $h_1 = 4.33$ ft.; $\frac{q}{\sqrt{g} h_1^{3/2}} = 0.0112$									
66	1.77	1.77	1.88	0.408	0.408	0.433	1.00	0.043	○
67	1.94	1.94	2.05	0.447	0.447	0.473	1.00	0.037	
68	2.06	2.06	2.15	0.484	0.484	0.496	1.00	0.034	
69	2.15	2.15	2.20	0.496	0.496	0.507	1.00	0.032	
70	2.20	2.20	2.25	0.507	0.507	0.518	1.00	0.031	
71	1.50	1.45	1.65	0.334	0.346	0.381	0.97	0.055	
72	1.09	0.90	1.35	0.207	0.251	0.311	0.82	0.089	
73	0.75	0.45	1.10	0.104	0.173	0.254	0.60	0.155	
*74	0.69	0.05	1.70	0.011	0.159	0.392	0.07	0.177	
$q = 0.453$ cfs/ft.; $h_1 = 4.10$ ft.; $\frac{q}{\sqrt{g} h_1^{3/2}} = 0.0096$									
75	1.53	1.53	1.64	0.373	0.373	0.400	1.00	0.042	○
76	1.81	1.81	1.86	0.441	0.441	0.453	1.00	0.033	
77	2.07	2.05	2.10	0.500	0.505	0.513	1.00	0.027	
78	2.20	2.20	2.24	0.536	0.536	0.546	1.00	0.024	
79	1.12	1.12	1.35	0.273	0.273	0.329	1.00	0.067	
80	0.64	0.32	1.00	0.078	0.156	0.244	0.50	0.157	
*81	0.62	0.04	1.40	0.010	0.151	0.341	0.07	0.163	

\*Free jet flow condition.



Data for Plots of Figures 4, 5 & 6

R = 1.2 ft.

Run	$h_2$ ft.	$h_b$ ft.	$h_s$ ft.	$h_b/h_1$	$h_2/h_1$	$h_s/h_1$	$h_b/h_2$	$\frac{q}{\sqrt{g} h_2^{3/2}}$	Symbol on Plot
$q = 0.430$ cfs/ft.; $h_1 = 5.95$ ft.; $\frac{q}{\sqrt{g} h_1^{3/2}} = 0.0052$									
96	3.00	3.00	3.00	0.504	0.504	0.504	1.00	0.015	■
97	2.50	2.45	2.53	0.411	0.419	0.424	0.98	0.019	
98	2.18	2.14	2.25	0.359	0.365	0.377	0.98	0.024	
99	1.60	1.48	1.75	0.249	0.268	0.293	0.93	0.038	
100	1.35	1.15	1.50	0.193	0.226	0.251	0.85	0.048	
101	1.03	0.75	1.20	0.126	0.173	0.201	0.73	0.072	
102	0.85	0.45	1.05	0.075	0.142	0.176	0.53	0.097	
*103	0.74	0.05	1.70	0.008	0.124	0.285	0.07	0.118	

$q = 1.280$  cfs/ft.;  $h_1 = 7.40$  ft.;  $\frac{q}{\sqrt{g} h_1^{3/2}} = 0.0112$

104	3.70	3.70	4.05	0.500	0.500	0.547	1.00	0.032	☒
105	3.30	3.30	3.65	0.446	0.446	0.493	1.00	0.038	
106	3.00	2.95	3.35	0.399	0.405	0.452	0.98	0.043	
107	2.65	2.55	3.00	0.345	0.358	0.405	0.96	0.052	
108	2.40	2.15	2.75	0.291	0.324	0.371	0.90	0.061	
109	2.10	1.75	2.60	0.237	0.284	0.351	0.83	0.074	
110	1.85	1.45	2.40	0.196	0.250	0.324	0.78	0.090	
111	1.60	1.10	2.10	0.149	0.216	0.284	0.69	0.111	
112	1.40	0.60	2.05	0.081	0.189	0.277	0.43	0.136	
113	1.25	0.30	1.95	0.041	0.169	0.264	0.24	0.161	
*114	1.20	0.08	3.40	0.001	0.162	0.459	0.07	0.172	

\*Free jet flow condition.

November 4, 1955

Tentative Program -  
Bucket-Type Energy Dissipator Characteristics

Hydraulic Lab., Lehigh University - for the Committee  
on Design, Hydraulics Division, A.S.C.E.

Major Objective:

Determination of parameter values for bucket-type  
dissipators of a specified class for direct use in design.

Outline of Program:

Phase II and III can be interchanged. Completion date  
for tests of Phase I is April 1, 1956. A one-foot wide steel  
flume with a sluice-gate operating under pressure will be used.  
At least 4 different values of  $R$  will be involved. (See  
attached sketch). Inasmuch as a  $45^\circ$  exit angle has been adopted  
by most designers as most efficient, the program will be  
restricted to this value, exclusively. The approach angle is  
of lesser importance, especially since  $h_1$  is to be referred  
to a point just upstream from the bucket roller. We feel that a  
 $45^\circ$  approach angle most nearly describes the condition for low to  
medium-head dams and that values of  $30^\circ$  to  $60^\circ$  would not materially  
affect the other parameters involved. We have a model at  $33^\circ$  on  
hand with which we can check, to some extent, this hypothesis.  
However, the present program will be restricted to an approach  
angle of  $45^\circ$ . We have observed in tests of bucket-type dissipators  
that so long as the downstream floor is no higher than the bucket  
invert the boil is not affected, inasmuch as the energy loss is  
restricted to the upper area of flow.

Phase I:

For a given  $R$ , hold  $h_2$  constant, vary  $h_1$  and  $Q$  for one  
set of runs. With various values of  $R/h_2$  see if suspicion that  
 $h_p = \phi(h_2)$  is correct (we hope). Proceed until a nomograph,  
table or plot for a range of each variable is attained. Values of  
 $x_s$  will be recorded for possible generalized use.

Phase II:

To attempt to delineate physical characteristics,  
including how much energy is dissipated in the bucket, in the  
boil, and beyond. An attempt will then be made to evaluate the  
motion by momentum relationships; determination of pressure-  
distribution along the bucket and vertical face below the bucket  
would be involved. Although this work may explain what takes  
place through the non-uniform flow sections, it is doubtful if a  
generalized equation supplanting the results of Phase I and suitable  
for design would be obtained.

Phase III:

For a typical range of the parameters of Phase I, replace the solid floor with stone and determine  $x$  (scour) and extent of scour. (For a given geometry we have noted that the scour distance is a function of  $h_1$ , only).

References: Bucket Dissipators

- a. Does Waterways Experiment Station Bulletin No. 37, "Hydraulic Models as an Aid to the Development of Design Criteris", represent the only data available from the Corps of Engineers? (For one radius, and definition of a free-jet condition).
- b. Is the Bureau of Reclamation Model Data on Grand Coulee Dam available? Are there other data?
- c. Mr. Rex A. Elder was so kind as to send us a copy of the Boone Project report. Unfortunately this was for a free-jet condition although they may have some data for submerged flow.
- d. The Discussion of A.S.C.E. Proceedings Separate 175, by Mr. Douma in Separate 384 is related but not directly applicable.

We have not had much opportunity to search the literature, as yet. Some basic information might be located in some of the classic works, such as those by Rehbock.